CANCER GENOMICS & PROTEOMICS *18*: 451-459 (2021)
doi:10.21873/cgp.20271

Efficacy of YAP1-gene Knockdown to Inhibit Alveolar-Epithelial-Cell Senescence and Alleviate Idiopathic Pulmonary Fibrosis (IPF)

WEI XU[1], WEIWEI SONG[2], YU WANG[1], YUMIN ZAN[1], MINGJIONG ZHANG[1], MIN LI[1], QIQING HUANG[1], WEIHONG ZHAO[1], YU SUN[3], ROBERT M. HOFFMAN[3] and JIANQING WU[1]

[1]*Key Laboratory of Geriatrics of Jiangsu Province, Department of Geriatrics, The First Affiliated Hospital of Nanjing Medical University, Nanjing, P.R. China;*
[2]*Department of Respiratory Medicine, Zhongnan Hospital of Wuhan University, Wuhan, P.R. China;*
[3]*Department of Surgery, UCSD, San Diego, CA, U.S.A.*

Abstract. *Background/Aim: The prevalence of idiopathic pulmonary fibrosis (IPF) increases with age and is associated with senescence of alveolar epithelial cells (AECs). AEC senescence in pulmonary cells mediates IPF. We herein aimed to determine if YAP1 gene knockdown, a member of the Hippo/YAP signal pathway, in the bleomycin (BLM)-induced mouse model of IPF, inhibits onset of senescence of AECs and alleviates IPF. Materials and Methods: Adeno-associated viruses (AAVs) expressing Yes-associated protein 1 (YAP1) short hairpin RNA (shRNA) were delivered into the lung of BLM-induced IPF mice via intratracheal injection, to knockdown the YAP1 gene in AECs. The mice were assigned to 4 groups: G1: control (normal mice); G2: IPF mice; G3: IPF + AAV/YAP1; G4: IPF + AAV/scramble. After 28 days, AECs were examined for senescence using H&E staining, Masson's trichrome Staining, senescence-associated ß-galactosidase (SA-β-gal) staining, western blotting and co-immunofluorescence staining, to determine the expression of YAP1, Smad-3 and p21, in order to determine the induction of senescence of ACEs. Results: The severity of IPF determined by H&E staining, Masson's staining and immunofluorescence (IF) staining was positively correlated with the senescence of AECs. Down-regulation of YAP1 expression of the Hippo-signaling pathway, determined by western blotting in AECs, alleviated pulmonary fibrosis as determined by Masson's staining. Down regulation of YAP1 expression reduced the senescence of AECs as determined by ß-galactosidase (SA-β-gal) staining, which alleviated the clinical symptoms of IPF mice, as determined by body weight and lung index. Conclusion: Down-regulation of YAP1 expression in AECs inhibited AEC senescence which is thought to be the cause of IPF. Therefore, future studies can focus on inhibiting YAP1 to effectively treat IPF.*

Correspondence to: Jianqing Wu, Key Laboratory of Geriatrics of Jiangsu Province, Department of Geriatrics, The First Affiliated Hospital of Nanjing Medical University, Nanjing, Jiangsu, 210029, PR China. Tel: +86 2568305150, e-mail: jwuny@njmu.edu.cn

Key Words: Alveolar epithelial cells, idiopathic pulmonary fibrosis, YAP gene knockdown, Hippo/YAP signal pathway, senescence.

Idiopathic pulmonary fibrosis (IPF) is a progressive, irreversible and fatal lung disease with multiple causal factors (1), with a median survival of only 2-3 years after diagnosis (2, 3). The pathogenesis of IPF is poorly understood but increases with age (4, 5), which is an independent risk factor. IPF is predominantly a disease of older adults (6). In patients >65 years, the estimated prevalence may be as high as 400 cases per 100,000 persons (7). Currently only two drugs, nintedanib and pirfenidone are approved for IPF. These drugs only slow the rate of lung function decline, but do not extend survival (8). Patients with IPF exhibit a greater risk for lung cancer development (9, 10). Lung tumors in patients with IPF develop preferentially in the periphery, immediately adjacent to fibrotic areas. This phenomenon is referred as "scar-cinoma"(11, 12). IPF is an independent, prognostic indicator of lung cancer (13). Cellular senescence of alveolar epithelial cells (AECs) in aged people comprises irreversible replicative arrest, apoptosis resistance, and acquisition of a senescence-associated secretory phenotype (SASP), which is regulated by a variety of cellular signal transduction pathways (14). Senescence has recently been shown to mediate IPF (15). In the present study, we knocked-down the Yes-associated protein 1 (YAP1) gene, a member of the HIPPO signaling

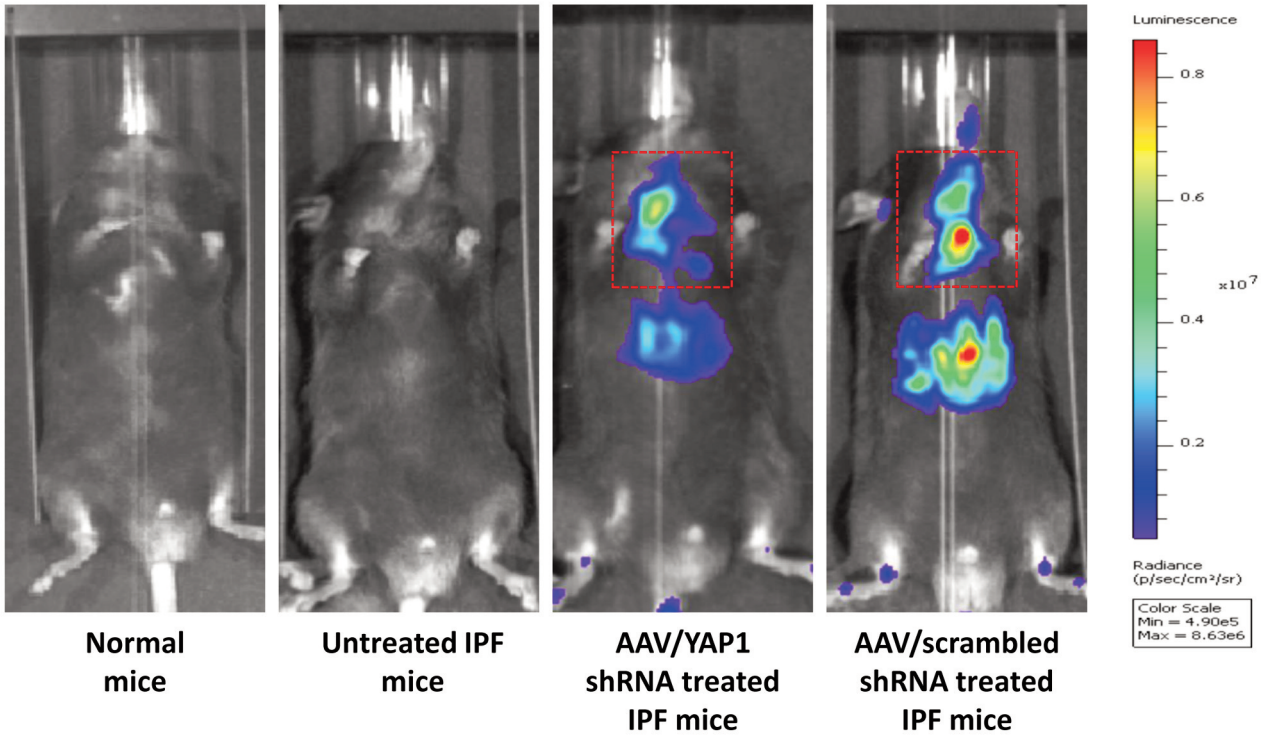

Figure 1. *Establishment of adeno-associated virus (AAV) delivery of either AAV/YAP1 shRNA OR YAP/scrambled shRNA, both linked to luciferase. Luciferin signal at the area of lung (red squares) was detected 4 weeks after delivery of the AAV.*

pathway (16), with YAP1/shRNA adeno-associated virus (AAV2/9) to inhibit senescence of AECs in a mouse model of bleomycin (BLM)-induced IPF.

Materials and Methods

Animals. A total of 32 C57BL/6 male mice, 20±2 g body weight, 5-6 weeks old, purchased from GemPharmatech Inc. (Nanjing, PR China) were used in the present study. All animals were bred at the Medical College of the Southeast University (Nanjing). All animals were maintained in a HEPA-filtered environment at a constant temperature of 25˚C and humidity of 60%. Cages, food, water and bedding were autoclaved.

AAV-YEP1 short hairpin RNA (shRNA)vector preparation. The AAV2/9 vector was purchased from Tran-medic BioTech (Nangjing, PR China). The 1.4 kb Cre.YAP1 shRNA (GCAUGAGCAGGUACAGCAUTT) or scrambled shRNA (TTCTCCGAACGTGTCACGT) was PCR-amplified from mouse genomic DNA, and cloned into the pAAV packaging plasmid together with the luciferase gene fragment to generate the pAAV-CMV-Luc-WPRE-U6-shRNA (YEP1-mus-1369) or pAAV-CMV-Luc-WPRE-U6-shRNA (scrambled) construct. The AAV2/9 -YEP vector and AAV2/9 scramble vectors were then produced by Tran-medic BioTech.

Establishment of the bleomycin (BLM)-induced IPF mouse model. Animals were anesthetized with continuous inhalation of 2.5% isoflurane. An approximately 1 cm longitudinal incision was made in the middle of the neck. The muscle was separated and the trachea was exposed. Ten μl (2.5 mg/kg) bleomycin (BLM) hydrochloride (Hanhui Pharmaceuticals Co., Zhejiang, PR China) was injected into the trachea using a 30 G insulin syringe (BD, Franklin, NJ, USA). When injecting BLM, the mice were kept in a vertical position and rotated several times to distribute BLM homogeneously. The incision was closed using a 5-0 nylon surgical sutures.

Grouping and treatment. Mice were randomly assigned to 4 groups with 8 mice in each group. G1: control (normal mice); G2: IPF mice; G3: IPF + AAV/YAP1 shRNA (2×10^{11} granular virus (GV) per mouse, endotracheal ×1); G4: IPF + AAV/scramble shRNA (2×10^{11} GV per mouse, endotracheal ×1). AAV treatment was started one week after BLM induction. Body weight of the mice was weighted twice per week using an electronic scale. After 6 weeks of initial treatment, 100 μl (1 mg) of D-luciferin potassium salt (Biovision, Milpitas, CA, USA) was injected intraperitoneally in each mouse. The luciferase signal was detected and captured using an IVIS® Spectrum (PerkinElmer, Waltham, MA, USA). At the end of experiment, all mice were euthanized and lungs were weight. Lung index [lung weight (g)/body weight (kg) ×100%] was calculated (17) and lung tissues were collected for histopathological analysis (please see below).

Histopathological analysis. Fresh lung samples were fixed in 10% formalin and embedded in paraffin before sectioning and staining. Tissue sections (4 μm) were deparaffinized in xylene and rehydrated in an ethanol series. Hematoxylin and eosin (H&E) staining was

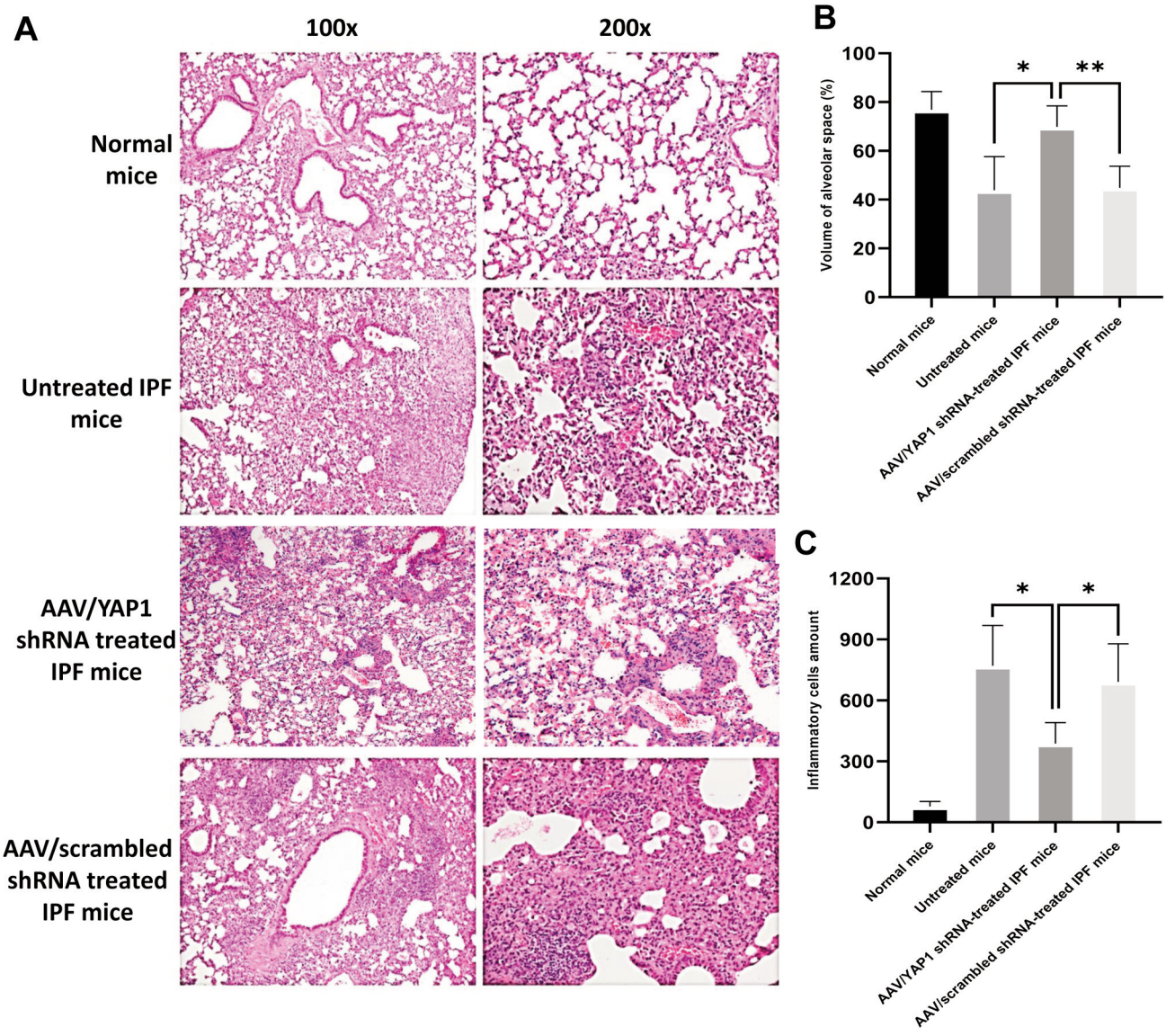

Figure 2. *Effect of YAP1 knockdown on pulmonary histology of IPF mice. (a) Typical images of H&E stained lung sections in each group; (b) Quantitation of relative alveolar area in each group; (c) Quantitation of inflammatory cells in each group. Data are represented as the mean±SD. *p<0.05, **p<0.01.*

used to determine the inflammatory changes in the YAP-knockdown and control lung tissue sections and Masson's trichrome staining was performed to determine the severity of pulmonary fibrosis. All images were captured using a CX31 microscope (Olympus Corp., Tokyo, Japan) with its software.

Western blotting. The level of YAP, p21 and Smad-3 in pulmonary tissues were measured using Western blotting. Tissue lysates were prepared using RIPA buffer with protease and phosphatase inhibiters (Beyotime, Shanghai, PR China). Protein was measured using a microplate reader (SPECTRA max Plus 384, Molecular Devices LLC., San Jose, CA, USA). Samples were run in a NOVEX 10–20% TRIS-glycine gel (Bio-Rad, Hercules, CA, USA). A Mini-Proten Tetra system (Bio-Rad) was used for dry transfer onto PVDF membranes (IPVH00010, MilliporeSigma, Burlington, MA, USA). Membranes were blocked using 5% bovine serum albumin (BSA) in TRIS-buffered saline, 0.1% tween 20 (TBST). Primary antibodies were diluted in 0.5% BSA/TBST. Western blots were quantified using ChemiDoc XRS+ System (Bio Rad) with its software, and normalized to glyceraldehyde-3-phosphate dehydrogenase (GAPDH).

Senescence assay. Senescence was quantified with colorimetric detection of senescence-associated ß-galactosidase (SA-β-gal) using a senescence detection kit (KeyGEN Biotech, Nangjing, PR China)

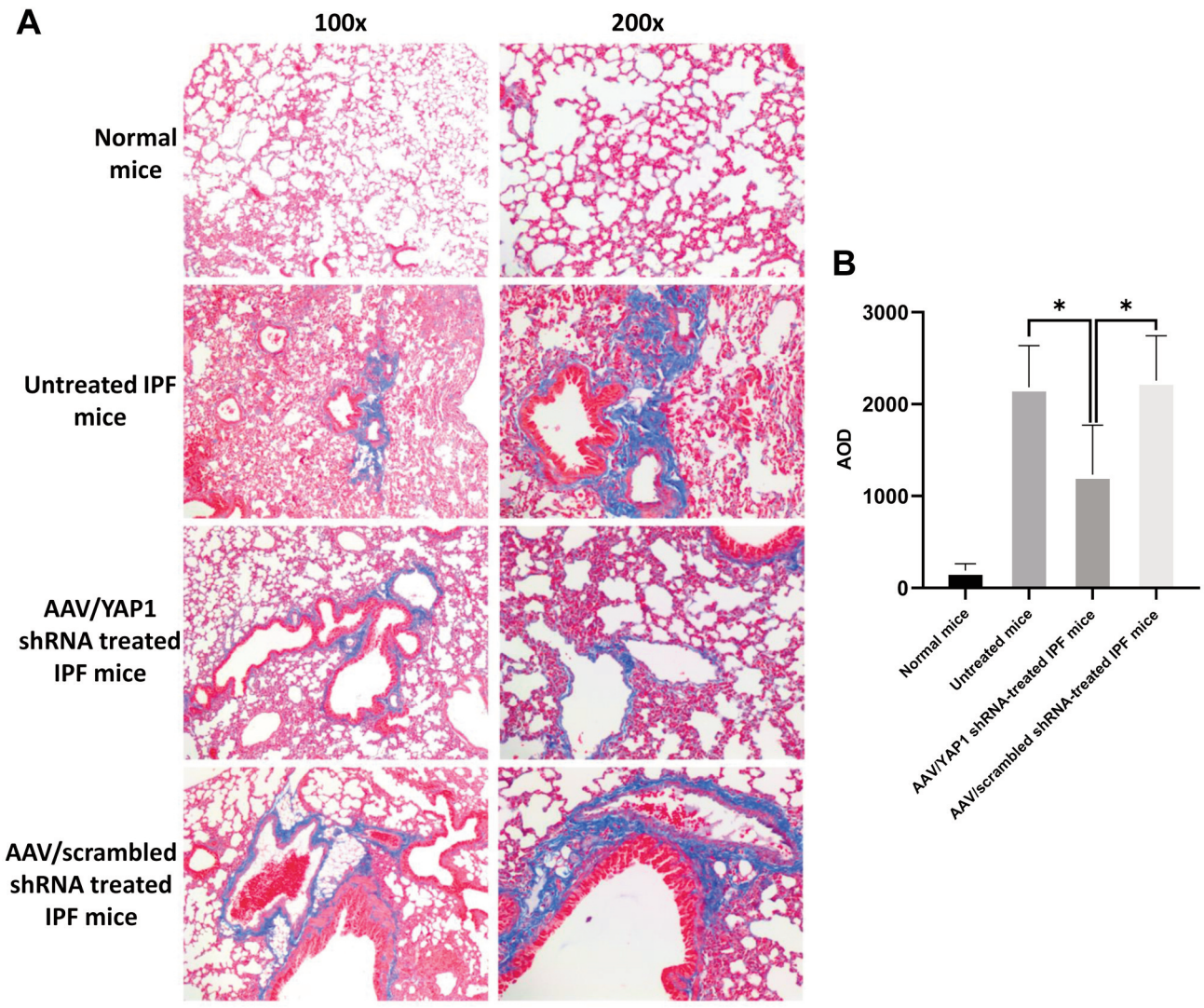

Figure 3. *Effect of YAP1 knockdown on AEC senescence (a) Masson's trichrome staining (blue) to identify fibrotic areas in H&E sections for all group; (b) The average optical density (AOD) of the fibrotic area was quantified in each group. Data are represented as the mean±SD. *p<0.05.*

according to the manufacturer's instructions. Tissue sections were prepared as described above. Slides were immersed in SA-β-gal solution (pH 6.0) overnight at 37˚C in the dark and were then fixed in 4% paraformaldehyde for 10 min followed by three washes in PBS, counterstained with nuclear fast red for 20-30 s and rinsed in running water for 2 min. Slides were then dehydrated in 95% ethanol and 100% ethanol followed by three treatments of xylene and mounted using mounting media. Images were captured using a CX31 microscope (Olympus Corp.) with its software.

Immunofluorescence (IF). To determine the expression of surfactant protein-C (SP-C), YAP, drosophila mothers against decapentaplegic -3 (Smad-3) and p21, immunofluorescence microscopy was performed using paraffin-embedded samples sectioned at 4-μm thickness. Slides were paraffinized with xylene and rehydrated using series of ethanol. After washing with phosphate buffer solution (PBS) 3 times for 5 min each time, TRIS- EDTA (pH 9.0) was used for antigen retrieval and washed with PBS 3 times for 5 min, each time. Samples were blocked with bovine serum albumin (BSA) for 20 min, BSA was removed and 50 μl diluted primary antibody was added and incubated at 4˚C overnight. After washing with PBS, 50 – 100 μl secondary antibody (1:200) and DAPI (1 μg/ml) were added and incubated for 2 hours in dark. Slides were washed with PBS and blocked using glycerin. Images were captured using an TE2000 inverted microscope (Nikon, Japan).

Primary antibodies specification: SP-C (ab90716, Abcam, Cambridge, UK); Smad-3 (sc-101154, Santa Cruz Biotech, Dallas, TX, USA); p21 (ab109199, Abcam); YEP1 (sc-101199, Santa Cruz Biotech) were used.

Statistical analysis. GraphPad Prism 9 software (GraphPad Inc., La Jolla, CA, USA) was used for data analysis. One-way variance

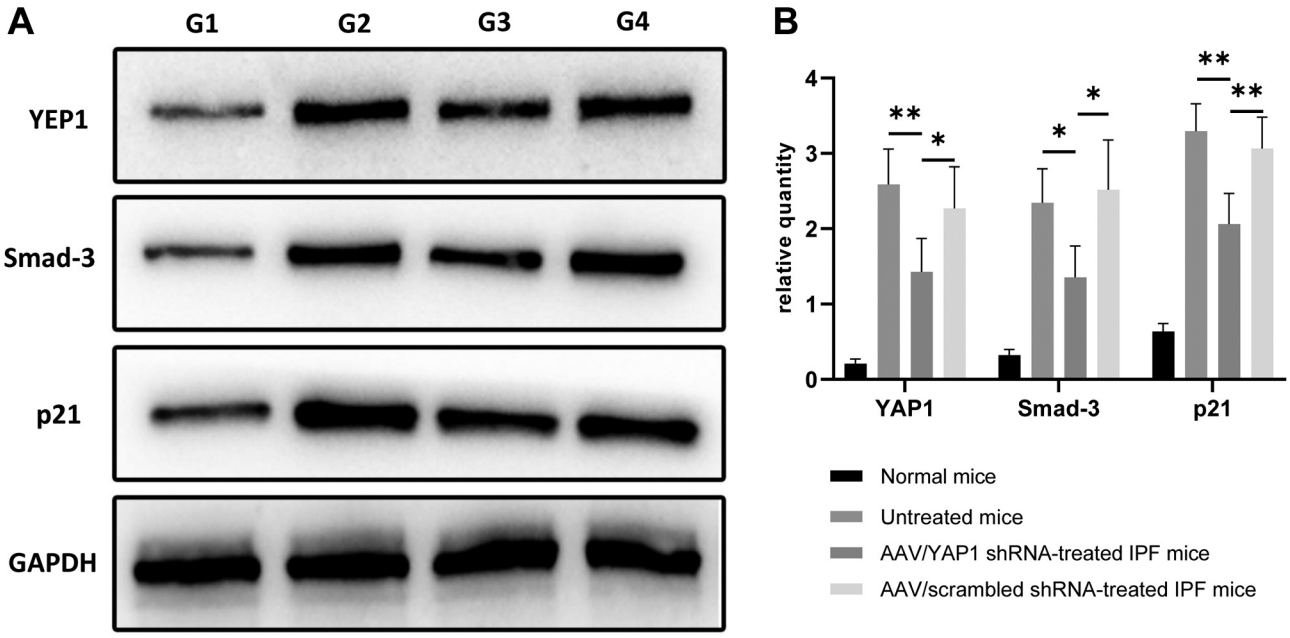

Figure 4. *Effect of YAP1 knockdown on biomarkers of fibrosis and senescence. (a) Western blotting analysis on the expression of YAP1, Smad-3 and p21 in each group. G1: Normal mice; G2: untreated IPF mice; G3: AAV/YAP1 shRNA treated IPF mice; G4: AAV/scrambled shRNA treated IPF mice. (b) Quantitative analysis of YAP1, Smad-3 and p21 expression in each group. Data are represented by the mean±SD. *p<0.05, **p<0.01.*

(ANOVA), followed by Turkey correction, were used to compare the significant-differences between the experimental groups. A *p*-value ≤0.05 was considered statistically significantly different.

Results

Knock-down of YAP1 inhibits IPF. Four weeks after treatment with luciferase-expressing AAV containing YAP1 shRNA, fluorescence signals were detected in both AAV/YAP1 and AAV/scramble-control treated mice (Figure 1), indicating that AAV successfully infected the lung in IPF mice.

H&E staining showed a significant increase of alveolar space in the AAV/YAP1 shRNA treated mice compared to control mice (p=0.033) and AAV/scrambled shRNA-treated mice (p=0.005). The amount of infiltrated inflammatory cells significantly decreased in the AAV/YAP1 shRNA-treated mice compared to untreated-control mice (p=0.010) and AAV/scrambled shRNA-treated mice (p=0.029) (Figure 2).

Masson's trichrome staining showed that mice treated with AAV/YAP1 shRNA had decreased collagen deposition compared to untreated mice (p=0.049) and AAV/scrambled shRNA treated mice (p=0.019) (Figure 3), indicating that YAP1 knockdown decreased fibrosis.

Knock-down of YAP1 inhibited the expression of YAP1, Smad-3 and p21 in IPF mice. The YAP1 protein expression was significantly decreased compared to the AAV/scramble (p=0.040) by AAV shRNA, indicating effective knockdown of the YAP1 gene.

The effects of YAP1 gene knockdown on pulmonary fibrosis marker (Smad-3) and senescence marker (p21) were determined. Both Smad-3 (p=0.046) and p21 (p=0.009) protein were significantly decreased by AAV shYAP1 compared to the AAV/scrambled shRNA (Figure 4). Thus, YAP1 knock down decreased senescence biomarkers in AECs in IPF mice.

Knock-down of YAP1 inhibited pulmonary cell senescence in IPF mice. To directly determine whether YAP1 knockdown inhibits AEC senescence in IPF mice,β-galactosidase staining was performed. Untreated IPF mice had significantly higher β-galactosidase expression in AECs compared with normal mice (p<0.01), indicating a positive correlation between AEC senescence and IPF (Figure 5). AAV/YAP1 shRNA significantly inhibited AECs senescence compared to the untreated mice (p=0.030) and AAV/scrambled shRNA-treated mice (p=0.033) (Figure 5).

Direct measurement of alveolar-epithelial cell (AEC) senescence in IPF mice. The expression of YAP, Smad-3 and p21 were significantly increased in AECs of IPF mice compared to normal mice. After knockdown of YAP1 by AAV/YAP1 shRNA, the expression of senescence biomarkers Smad-3 and p21 decreased in the ACEs (Figure 6).

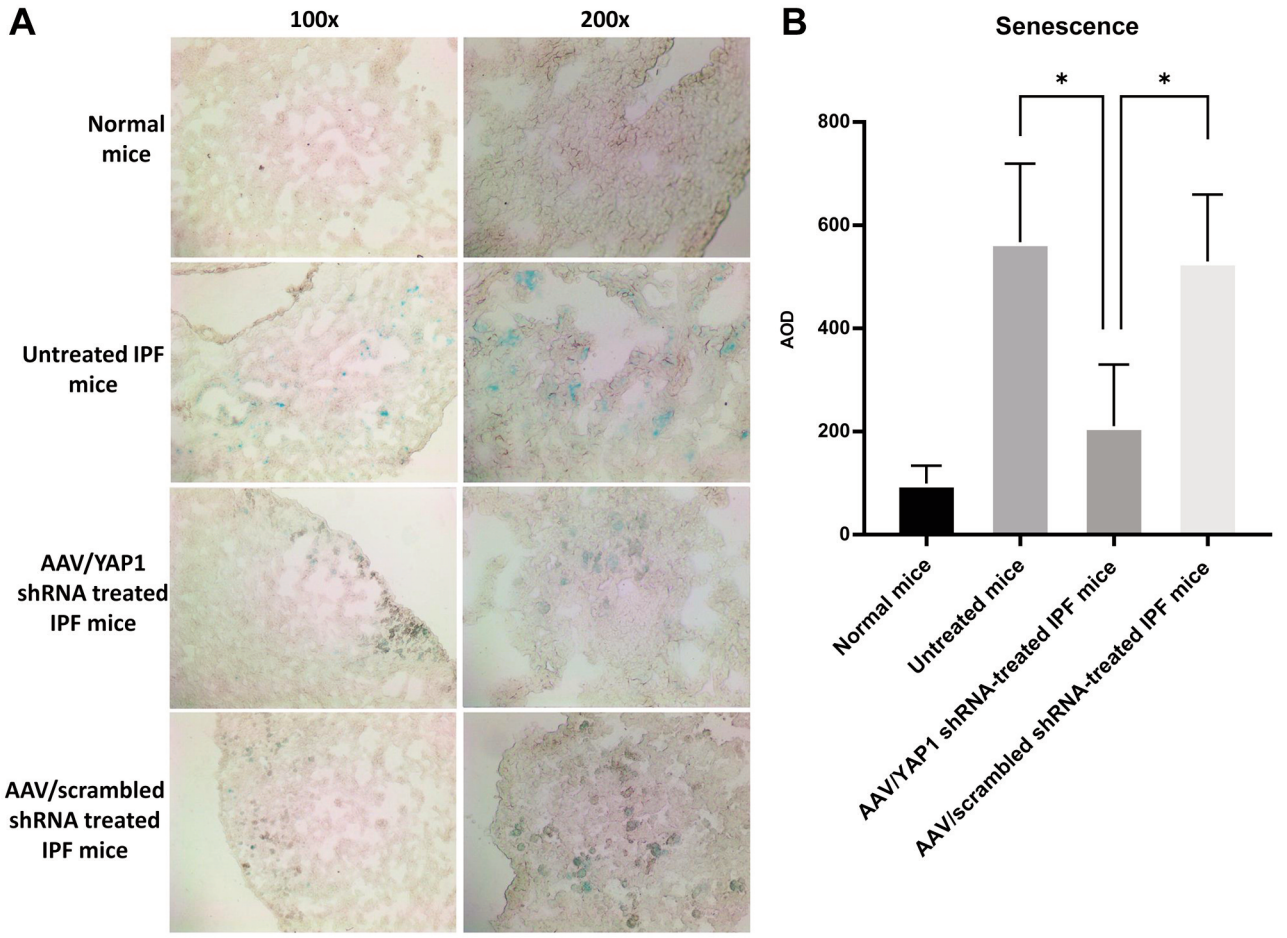

Figure 5. *Effect of YAP1 knockdown on AEC senescence. (a) Senescence increase β-galactosidase activity (blue staining). (b) Quantitative analysis of senescence by average optical density (AOD) in each group. Data are represented as the mean±SD. *p<0.05, **p<0.01.*

Effect of YAP1 knockdown on body weight and lung index in IPF mice. BLM caused significant body weight loss by the end of the study in all IPF model groups compared to normal mice ($p<0.05$). AAV/shYAP1-treated mice (G3) had increased body weight compared to untreated mice (G2) ($p=0.043$) and AAV/scrambled shRNA-treated mice ($p=0.017$) (Figure 7a).

Untreated IPF mice had a significantly increased lung index compared to normal mice ($p<0.05$). AAV/YAP1 shRNA (G3) significantly improved the lung index compared to untreated IPF mice (G2) ($p=0.001$) and AAV/scrambled shRNA-treated mice (G4) ($p=0.001$) (Figure 7b).

Discussion

IPF is a recalcitrant fatal disease, causing patients to suffocate to death. The two approved drugs for IPF appear only to be palliative (18). It has been suggested that senescence of AEC is causal to IPF of AEC: the elevated abundance of senescence biomarkers in IPF lung, and their expression level is positively correlated with disease severity (15). The present result implicates the YAP1 gene of the Hippo/YAP signaling pathway as a causal gene for AEC senescence.

The present report has shown that knockdown of YAP1 decreased the expression of Smad-3 in AECs of IPF mice. It has been previously reported that the development of IPF is a Smad-3-dependent process which can increase collagen deposition in AEC (19) resulting in the onset of IPF. The expression of p21, a cellular senescence marker, was significantly increased in the AECs of IPF and decreased after YAP1 knockdown. After AAV/YAP1 knockdown treatment, senescent AECs decreased. Thus down-regulation of YAP1 expression of the Hippo signaling pathway in AECs inhibits AEC senescence and alleviates IPF.

In future experiments, we will establish an animal model of lung cancer combined with IPF to investigate the effect

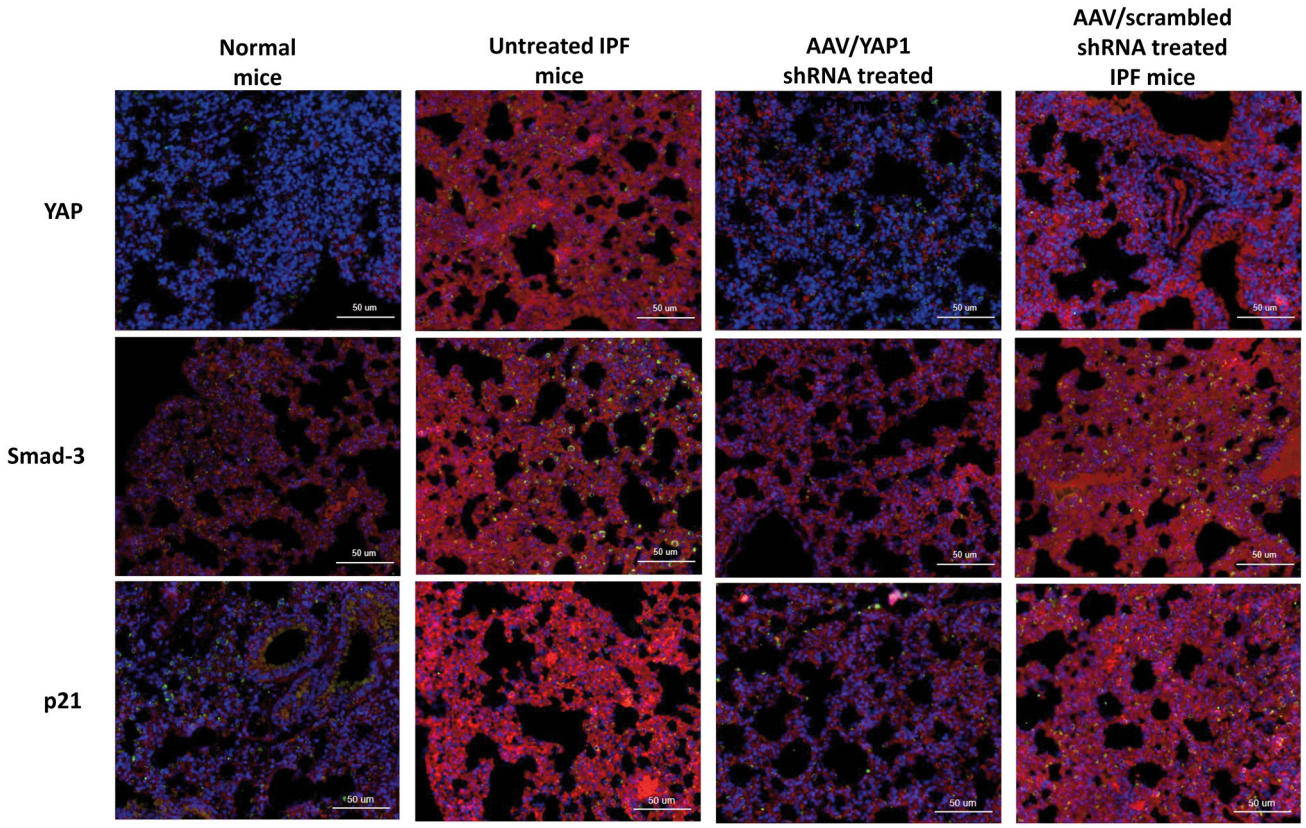

Figure 6. *Effect of YAP1 knockdown on fibrotic and senescence biomarkers. Red color is positive immunostaining of YAP, Smad-3 and p21. Blue color is DAPI.*

of the Hippo signal pathway in IPF-induced scar-cinoma and subsequent lung cancer.

Conflicts of Interest

The Authors have no conflicts to declare.

Authors' Contributions

Wei Xu and Jianqing Wu designed the study; Weiwei Song, Yu Wang, Yumin Zan, Min Li and Mingjiong Zhang performed the experiments; Yu Sun and Qiqing Huang analyzed the data; Wei Xu and Weihong Zhao drafted the manuscript; Robert M. Hoffman revised the manuscript; Jianqing Wu administrated and supervised the study.

Acknowledgements

This work was supported by Jiangsu Provincial Key Discipline of Medicine: ZDXKA2016003; The National Natural Science Foundation of China: 81871100, 81871115; Scientific Research Project of Jiangsu Provincial Health Commission: H2019036; The Jiangsu Province's Medical Talents Program: LGY2017071.

References

1 Chua F, Sly PD and Laurent GJ: Pediatric lung disease: From proteinases to pulmonary fibrosis. Pediatr Pulmonol *39(5)*: 392-401, 2005. PMID: 15786437. DOI: 10.1002/ppul.20171

2 Bou Ghanem EN: mSphere of Influence: Adenosine in Host Defense against Bacterial Pneumonia-Friend or Foe? mSphere *4(4)*: e00326-19, 2019. PMID: 31292232. DOI: 10.1128/mSphere.00326-19

3 From the American Association of Neurological Surgeons (AANS), American Society of Neuroradiology (ASNR), Cardiovascular and Interventional Radiology Society of Europe (CIRSE), Canadian Interventional Radiology Association (CIRA), Congress of Neurological Surgeons (CNS), European Society of Minimally Invasive Neurological Therapy (ESMINT), European Society of Neuroradiology (ESNR), European Stroke Organization (ESO), Society for Cardiovascular Angiography and Interventions (SCAI), Society of Interventional Radiology (SIR), Society of NeuroInterventional Surgery (SNIS), and World Stroke Organization (WSO), Sacks D, Baxter B, Campbell BCV, Carpenter JS, Cognard C, Dippel D, Eesa M, Fischer U, Hausegger K, Hirsch JA, Shazam Hussain M, Jansen O, Jayaraman MV, Khalessi AA, Kluck BW, Lavine S, Meyers PM, Ramee S, Rüfenacht DA, Schirmer CM and Vorwerk D: Multisociety consensus quality improvement revised consensus

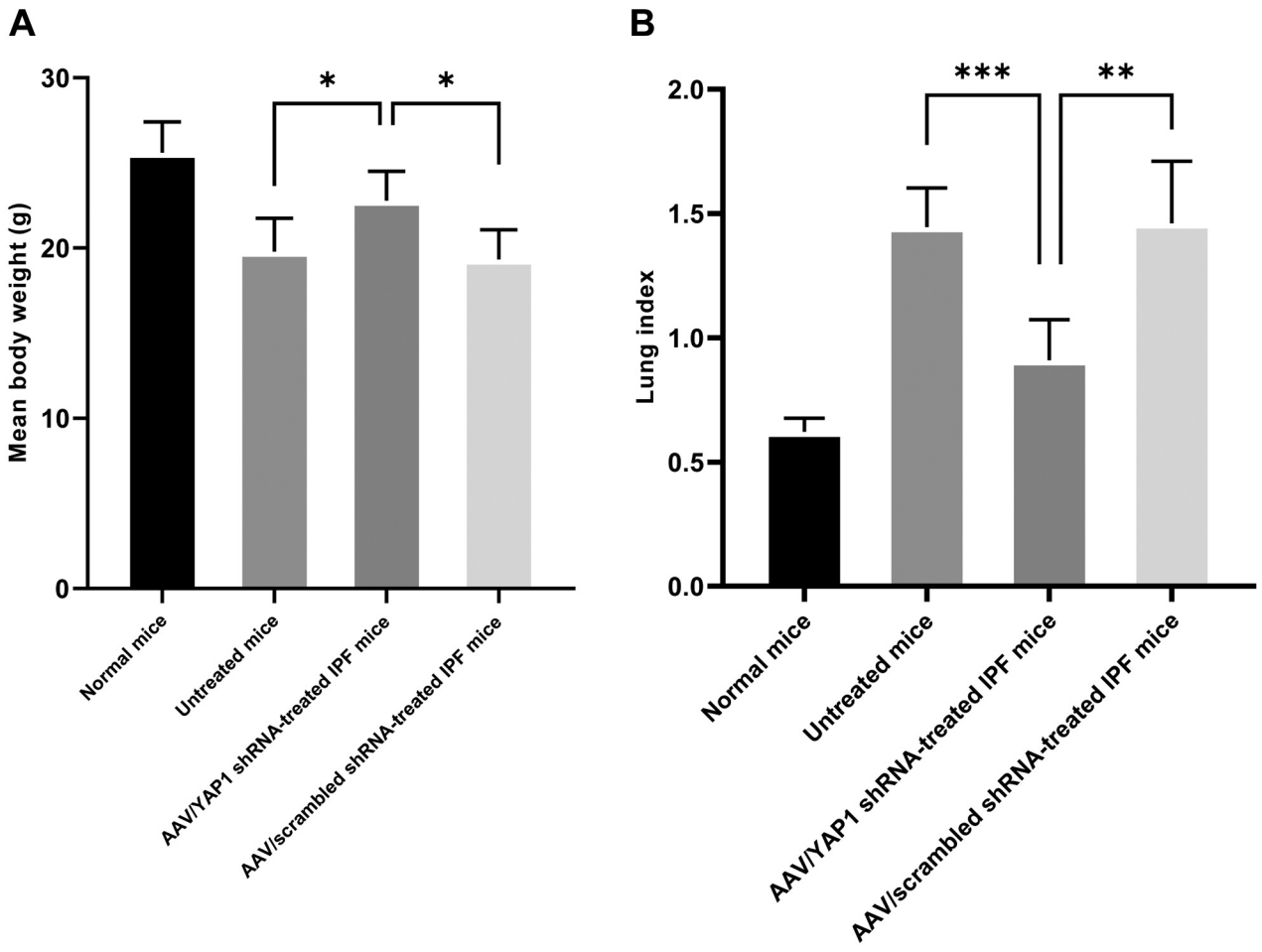

Figure 7. *Effect of YAP1 knockdown on body weight and lung index in IPF mice. (a) Mean body weight in each group at the end of the study (day 28); (b) Mean lung index in each group at the end of the study (day 28). Data are represented as the mean±SD. *p<0.05, **p<0.01, ***p<0.001.*

statement for endovascular therapy of acute ischemic stroke. Int J Stroke *13(6)*: 612-632, 2018. PMID: 29786478. DOI: 10.1177/1747493018778713

4 Zhu T, Ma Z, Wang H, Jia X, Wu Y, Fu L, Li Z, Zhang C and Yu G: YAP/TAZ affects the development of pulmonary fibrosis by regulating multiple signaling pathways. Mol Cell Biochem *475(1-2)*: 137-149, 2020. PMID: 32813142. DOI: 10.1007/s11010-020-03866-9

5 Li Y, Liang J, Yang T, Monterrosa Mena J, Huan C, Xie T, Kurkciyan A, Liu N, Jiang D and Noble PW: Hyaluronan synthase 2 regulates fibroblast senescence in pulmonary fibrosis. Matrix Biol *55*: 35-48, 2016. PMID: 26987798. DOI: 10.1016/j.matbio.2016.03.004

6 Castriotta RJ, Eldadah BA, Foster WM, Halter JB, Hazzard WR, Kiley JP, King TE Jr, Horne FM, Nayfield SG, Reynolds HY, Schmader KE, Toews GB and High KP: Workshop on idiopathic pulmonary fibrosis in older adults. Chest *138(3)*: 693-703, 2010. PMID: 20822991. DOI: 10.1378/chest.09-3006

7 Raghu G, Chen SY, Yeh WS, Maroni B, Li Q, Lee YC and Collard HR: Idiopathic pulmonary fibrosis in US Medicare beneficiaries aged 65 years and older: Incidence, prevalence, and survival, 2001-11. Lancet Respir Med *2(7)*: 566-572, 2014. PMID: 24875841. DOI: 10.1016/S2213-2600(14)70101-8

8 Mora AL, Rojas M, Pardo A and Selman M: Emerging therapies for idiopathic pulmonary fibrosis, a progressive age-related disease. Nat Rev Drug Discov *16(11)*: 755-772, 2017. PMID: 28983101. DOI: 10.1038/nrd.2017.170

9 Archontogeorgis K, Steiropoulos P, Tzouvelekis A, Nena E and Bouros D: Lung cancer and interstitial lung diseases: A systematic review. Pulm Med *2012*: 315918, 2012. PMID: 22900168. DOI: 10.1155/2012/315918

10 Bouros D, Hatzakis K, Labrakis H and Zeibecoglou K: Association of malignancy with diseases causing interstitial pulmonary changes. Chest *121(4)*: 1278-1289, 2002. PMID: 11948064. DOI: 10.1378/chest.121.4.1278

11 Tzouvelekis A, Gomatou G, Bouros E, Trigidou R, Tzilas V and Bouros D: Common pathogenic mechanisms between idiopathic

pulmonary fibrosis and lung cancer. Chest *156(2)*: 383-391, 2019. PMID: 31125557. DOI: 10.1016/j.chest.2019.04.114

12 Horowitz JC, Osterholzer JJ, Marazioti A and Stathopoulos GT: "Scar-cinoma": Viewing the fibrotic lung mesenchymal cell in the context of cancer biology. Eur Respir J *47(6)*: 1842-1854, 2016. PMID: 27030681. DOI: 10.1183/13993003.01201-2015

13 Koyama N, Iwai Y, Nagai Y, Aoshiba K and Nakamura H: Idiopathic pulmonary fibrosis in small cell lung cancer as a predictive factor for poor clinical outcome and risk of its exacerbation. PLoS One *14(8)*: e0221718, 2019. PMID: 31442290. DOI: 10.1371/journal.pone.0221718

14 Kirkland JL and Tchkonia T: Cellular Senescence: A translational perspective. EBioMedicine *21*: 21-28, 2017. PMID: 28416161. DOI: 10.1016/j.ebiom.2017.04.013

15 Schafer MJ, White TA, Iijima K, Haak AJ, Ligresti G, Atkinson EJ, Oberg AL, Birch J, Salmonowicz H, Zhu Y, Mazula DL, Brooks RW, Fuhrmann-Stroissnigg H, Pirtskhalava T, Prakash YS, Tchkonia T, Robbins PD, Aubry MC, Passos JF, Kirkland JL, Tschumperlin DJ, Kita H and LeBrasseur NK: Cellular senescence mediates fibrotic pulmonary disease. Nat Commun *8*: 14532, 2017. PMID: 28230051. DOI: 10.1038/ncomms14532

16 Chen Y, Zhao X, Sun J, Su W, Zhang L, Li Y, Liu Y, Zhang L, Lu Y, Shan H and Liang H: YAP1/Twist promotes fibroblast activation and lung fibrosis that conferred by miR-15a loss in IPF. Cell Death Differ *26(9)*: 1832-1844, 2019. PMID: 30644438. DOI: 10.1038/s41418-018-0250-0

17 Gungor H, Ekici M, Onder Karayigit M, Turgut NH, Kara H and Arslanbas E: Zingerone ameliorates oxidative stress and inflammation in bleomycin-induced pulmonary fibrosis: Modulation of the expression of TGF-β1 and iNOS. Naunyn Schmiedebergs Arch Pharmacol *393(9)*: 1659-1670, 2020. PMID: 32377772. DOI: 10.1007/s00210-020-01881-7

18 Barratt SL, Creamer A, Hayton C and Chaudhuri N: Idiopathic pulmonary fibrosis (IPF): An overview. J Clin Med *7(8)*:201, 2018. PMID: 30082599. DOI: 10.3390/jcm7080201

19 Verrecchia F, Chu ML and Mauviel A: Identification of novel TGF-beta /Smad gene targets in dermal fibroblasts using a combined cDNA microarray/promoter transactivation approach. J Biol Chem *276(20)*: 17058-17062, 2001. PMID: 11279127. DOI: 10.1074/jbc.M100754200

Received February 1, 2021
Revised February 16, 2021
Accepted March 9, 2021